Analysis of localization effect in blue-violet light emitting InGaN/GaN multiple quantum wells with different well widths*

Xiang Li(李翔)[1], De-Gang Zhao(赵德刚)[1,2,†], De-Sheng Jiang(江德生)[1], Jing Yang(杨静)[1], Ping Chen(陈平)[1], Zong-Shun Liu(刘宗顺)[1], Jian-Jun Zhu(朱建军)[1], Wei Liu(刘炜)[1], Xiao-Guang He(何晓光)[1], Xiao-Jing Li(李晓静)[1], Feng Liang(梁锋)[1], Jian-Ping Liu(刘建平)[3], Li-Qun Zhang(张立群)[3], Hui Yang(杨辉)[1,3], Yuan-Tao Zhang(张源涛)[4], Guo-Tong Du(杜国同)[4], Heng Long(龙衡)[5], and Mo Li(李沫)[5]

[1] *State Key Laboratory on Integrated Optoelectronics, Institute of Semiconductors, Chinese Academy of Sciences, Beijing* 100083, *China*
[2] *University of Chinese Academy of Sciences, Beijing* 100049, *China*
[3] *Suzhou Institute of Nano-tech and Nano-bionics, Chinese Academy of Sciences, Suzhou* 215125, *China*
[4] *State Key Laboratory on Integrated Optoelectronics, College of Electronic Science and Engineering, Jilin University, Changchun* 130023, *China*
[5] *Microsystem & Terahertz Research Center, Chinese Academy of Engineering Physics, Chengdu* 610200, *China*

(Received 13 May 2016; revised manuscript received 9 October 2016; published online 30 November 2016)

Four blue-violet light emitting InGaN/GaN multiple quantum well (MQW) structures with different well widths are grown by metal–organic chemical vapor deposition. The carrier localization effect in these samples is investigated mainly by temperature-dependent photoluminescence measurements. It is found that the localization effect is enhanced as the well width increases from 1.8 nm to 3.6 nm in our experiments. The temperature induced PL peak blueshift and linewidth variation increase with increasing well width, implying that a greater amplitude of potential fluctuation as well as more localization states exist in wider wells. In addition, it is noted that the broadening of the PL spectra always occurs mainly on the low-energy side of the PL spectra due to the temperature-induced band-gap shrinkage, while in the case of the widest well, a large extension of the spectral curve also occurs in the high energy sides due to the existence of more shallow localized centers.

Keywords: InGaN/GaN multiple quantum wells, localization effect, well thickness

PACS: 78.66.Fd, 78.67.De, 85.60.Jb, 78.60.Fi **DOI:** 10.1088/1674-1056/26/1/017805

1. Introduction

InGaN/GaN multiple quantum wells (MQWs) have been extensively used as active regions in high luminescent efficiency light emitting diode (LED) and laser diode (LD) devices.[1–7] Despite the high dislocation densities ($\sim 10^7$–10^8 cm^{-2}) in epitaxially grown *c*-plane GaN[8] and the strong quantum confined Stark effect (QCSE) in InGaN/GaN QWs,[9] these devices exhibit very surprisingly high luminescence efficiencies in blue-violet emitting InGaN/GaN MQWs. The carrier localization effect is accepted as an important luminescence-enhancement mechanism.[10,11] In general, it is believed that the localization effect can give rise to a reduction of carrier migration into non-radiative centers, and enlarges the matrix element for optical transition by attracting carriers within the same localized sites.[9] As a result, in spite of the existence of a large number of defects, the luminescence efficiency of the InGaN/GaN MQWs is significantly enhanced. The investigation about the influences of the QW-related parameters on the luminescence of MQW structures is reported.[12–17] Even so, it is believed that the effects of the QW width on the localization effect especially in the blue-violet light emitting InGaN/GaN MQW structures should be further studied by analyzing the photoluminescence spectra as thoroughly as possible for improving the device performances.

In this work, the dependence of the localization effect on the well width is mainly investigated by the aid of temperature-dependent photoluminescence (PL) measurements. The parameters obtained from the temperature-dependent PL spectra including the peak intensity, the full width at half maximum (FWHM), and the shape are analyzed in detail. In order to study the influence of the InGaN QW width, four InGaN/GaN MQW samples with varying well thickness are grown by using a metal–organic chemical vapor deposition (MOCVD) system. It is found that the potential fluctuation is increased with increasing well thickness. Greater amplitudes of potential fluctuations as well as more localization states exist in wider wells. It is also found that the PL peak intensity has a non-monotonous variation as the well width increases, which is believed due to the comprehensive effects of the localization effect, QCSE, the influence of the material quality of the InGaN layers, and the laser-absorbing active region volume.

*Project supported by the National Key Research and Development Program of China (Grant No. 2016YFB0401801), the National Natural Science Foundation of China (Grant Nos. 61674138, 61674139, 61604145, 61574135, 61574134, 61474142, 61474110, 61377020, and 61376089), Science Challenge Project, China (Grant No. JCKY2016212A503), and One Hundred Person Project of the Chinese Academy of Sciences.

†Corresponding author. E-mail: dgzhao@red.semi.ac.cn

© 2017 Chinese Physical Society and IOP Publishing Ltd

2. Experimental procedures

The four InGaN/GaN MQW samples with different well widths studied in this work were grown in an AIXTRON close-coupled showerhead 3×2 in low-pressure vertical reactor MOCVD system on *c*-plane sapphire substrates spinning at 100 rpm. Trimethylindium, trimethylaluminum, and ammonia (NH_3) were used as the source materials for In, Al, and N, respectively. The precursor of Ga was trimethylgallium (TMGa) everywhere, except in the InGaN/GaN MQW region growth triethylgallium (TEGa) was used. Silane (SiH_4) and bicyclopentadienyl magnesium (Cp_2Mg) were used as the n-type and the p-type doping precursors, respectively. The substrates were initially treated in a ambient H_2 at 1137 °C, followed by the growth of a 25 nm thick, low-temperature GaN buffer layer at 550 °C and a 1.5 μm thick layer of Si-doped n-type GaN at high temperature under low pressure. Three periods of InGaN/GaN MQWs with well and barrier growth temperatures of 730 °C and 830 °C were grown on the GaN template, followed by a 150 nm Mg-doped p-type GaN cladding layer to fabricate the MQW structures. All samples were grown in rapid succession under identical conditions except of the growth time of the InGaN well layers. The growth time of the QWs was employed as a modulating parameter to change the width of the InGaN layers in the MQW structures. The growth time of each individual well layer was 120 s, 160 s, 200 s, and 240 s for these four samples, labeled as samples S120, S160, S200, and S240, respectively.

Temperature-dependent PL measurements were carried out with the 325-nm line of a He–Cd laser at an excitation density of 0.8 W/cm^2 to investigate the localization effect, and the temperature was controlled to change from 30 K to 300 K using a closed-cycle refrigerator of CTI Cryogenics. The detected PL spectral lines were fitted by Gaussian functions to eliminate the influence induced by the Fabry–Perot interference fringes for analyzing the accurate peak energy and FWHM.

3. Results and discussion

In fact, the investigation of the InGaN/GaN MQW structures with only three periods is mainly for the purpose of optimizing the QW growth of GaN based LDs. Unfortunately, because of the small QW number and the additional thick layer on the top of the active region, the intensity of the MQW layer peak signal in high resolution x-ray diffraction (HRXRD) is too low to measure,[18] and the indium mole fraction and the InGaN QW width cannot be exactly determined for these four samples. To obtain the InGaN well layer growth rate, an extra 37.5 nm-thick InGaN layer was grown on a GaN template using the same growth conditions with the InGaN QW of these samples, and taken as a reference sample. The thickness of the reference sample was controlled by an *in situ* monitoring system installed in the MOCVD system (data not shown here). The growth time of the 37.5 nm-thick reference sample was recorded as 2500 s and thus the average growth rate of QW was calculated to be 0.015 nm/s. According to the growth rate, the estimated QW width of samples S120, S160, S200, and S240 is around 1.8 nm, 2.4 nm, 3 nm, and 3.6 nm, respectively.

The PL spectra of these four samples measured at room temperature are plotted in Fig. 1. The optical parameters extracted from the PL spectra, including peak energy, peak intensity, and FWHM, are listed in Table 1. From Table 1, it can be seen that the PL peak emission energy of the MQWs redshifts from 3.09 eV to 2.89 eV with increasing well width from 1.8 nm to 3.6 nm, which can be ascribed to the quantum confinement effect and QCSE.[19] As for the PL peak and integrated intensity, they exhibit a similar and non-monotonic variation trend with increasing QW width. Specifically, the PL intensity is remarkably increased from 0.4 to 7.8 when the well width is increased to 3 nm from 1.8 nm. However, it is reduced to 3.8 when the well width reaches 3.6 nm. The variation of the peak and integrated intensity could be influenced by QCSE, the material quality, the laser-absorbing material volume, and the localization effect. It is known that as the well width increases, QCSE is enhanced and the wave function overlap between electrons and holes is reduced, leading to the lowered luminescence efficiency. Meanwhile, the material quality including the interface roughness is degraded due to the increased InGaN well width, thus further deteriorating the optical quality.[8,9] Nevertheless, the peak intensity is still enhanced when the well width is increased to 3 nm. This is at least partly attributed to the increased laser-absorbing material volume, and thus the number of photo-generated carriers in the active regions, as well as the PL intensity, is increased. As for the FWHM, as the well width increases, it increases monotonically from 65 meV to 98 meV. Also, it is believed that both FWHM and PL peak intensity are greatly affected by the localization effect in the well layers. Therefore, it is very necessary to study the influences of the well-thickness dependent localization effect on the optical property of InGaN/GaN QWs.

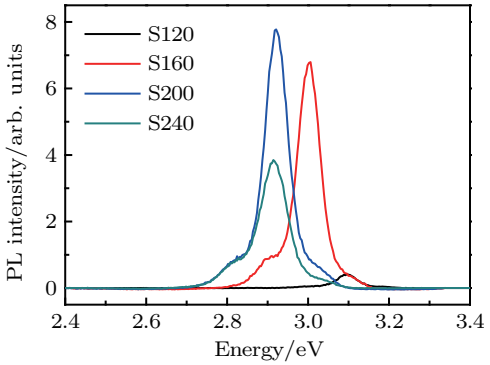


Fig. 1. (color online) The room temperature PL spectra of the InGaN/GaN MQW samples S120, S160, S200, and S240.

Table 1. The optical parameters extracted from the PL spectra of all samples, including peak energy, peak intensity, and FWHM.

Sample	Well width/nm	Peak energy/eV	Peak intensity/arb. units	Integrated intensity/arb. units	FWHM /meV
S120	1.8	3.09	0.4	1.3	65.0
S160	2.4	2.98	6.8	9.6	75.4
S200	3	2.92	7.8	16.2	79.9
S240	3.6	2.89	3.8	6.0	98.0

The PL spectra of the InGaN/GaN MQW structures of the four samples are measured under the same conditions when the temperature increases from 30 K to 300 K. The internal quantum efficiency (IQE) is often obtained through temperature-dependent PL measurement,[20] and here is defined as the ratio of the integrated PL intensity at 300 K and 30 K (data not shown here). The IQE is calculated as 1.5%, 7.2%, 9.5%, and 3.8% for samples S120, S160, S200, and S240, respectively, which is in accordance with their PL intensity. The PL peak energy as a function of temperature is depicted in Fig. 2 for all samples. Since a relatively low excitation power is used in our PL measurements, an anomalous S-shaped red-/blue-/redshift of the temperature-dependent PL peak energy can be observed. In general, the S-shaped behavior in the temperature dependence of the peak emission energy is linked to the existence of potential fluctuations and carrier localization–delocalization process.[21] The detailed explanation about the S-shaped behavior in the temperature dependence of the peak energy is as follow.[22] At very low temperature of 30 K, the photo-generated carriers do not have sufficient thermal energy, and cannot relax down to the separately-distributed lower energy level states, so they are randomly distributed in the potential minima. As the temperature rises, the weakly localized carriers are thermally activated and can relax down into lower localized states via hopping, leading to an initial redshift of the PL peak. The subsequent blueshift of the PL peak is the result of the Boltzmann occupation of the localized states.[23] More and more carriers are thermally excited out from the deepest localization centers, and may come into the shallower localization centers. In fact, the temperature induced band-gap shrinkage occurs as soon as the temperature rises. The band-gap shrinkage starts to dominate in the relatively high temperatures, causing another redshift. Based on the explanation about the S-shaped behavior, it can be summarized that the temperature-induced blueshift of the emission energy at intermediate temperatures indicates the fluctuation range of the localization states, and it is the fingerprint of the localization effect.[13] As seen from Fig. 2, the range of blueshift for samples S120, S160, S200, and S240 is calculated to be about 3 meV, 3 meV, 10 meV, and 14 meV, respectively. Obviously, as the well width increases, the blueshift increases, which indicates that the distribution of the localization states is wider in thicker QWs. Therefore, it can be inferred that the localization effect may be enhanced with increasing well width.

The band-tail model is always employed to investigate the localization degree.[24] In InGaN QWs, band tail states can appear in an electron energy diagram caused by the disorders in InGaN/GaN QWs, introduced by either strong compositional non-uniformity of InGaN or QW thickness fluctuations. The tail states can provide the energy levels lower than the nominal band edge to confine the localized carriers. If a Gaussian-like distribution of the density of band tail states for the conduction and valence bands is assumed, the temperature-dependent emission energy could be described by the following expression:[13]

$$E_{\mathrm{g}}(T) = E_{\mathrm{g}}(0) - \frac{\alpha T^2}{T+\beta} - \frac{\sigma^2}{K_{\mathrm{B}}T}, \tag{1}$$

where $E_{\mathrm{g}}(0)$ describes the energy gap at zero temperature, α and β are known as Varshini's fitting parameters, and σ indicates the broadening effect of the Gaussian-like band tail states into the nominally forbidden band. Therefore, the value of σ can reflect the degree of localization effect, and a larger σ is often corresponding to a stronger localization effect. By fitting Eq. (1) to the curves, the parameter σ is obtained as 11.4 meV, 11.9 meV, 15.6 meV, and 16.5 meV for samples S120, S160, S200, and S240, respectively. It is found that σ is larger for the samples with wider QWs, which implies that the localization effect in wider QW is stronger. Finally, as mentioned before, the localization effect can be a reason responsible for the increasing temperature-induced blueshift of the PL peak with increasing well width as shown in Fig. 2.

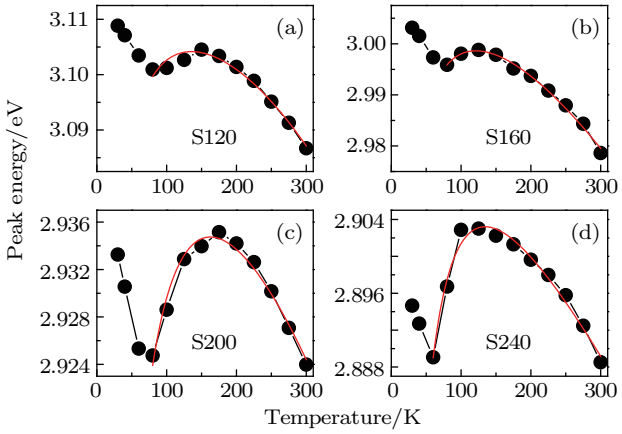


Fig. 2. (color online) The PL peak energy as a function of temperature for samples (a) S120, (b) S160, (c) S200, and (d) S240. The red solid lines are the fitting curves according to Eq. (1).

To further study the relation of potential fluctuations with the well width, the temperature-dependent FWHM of all samples is measured as demonstrated in Fig. 3, where the FWHM of the PL peak represents the broadening and/or narrowing effect of the PL spectra, providing information about the distribution of the localization states and the related potential fluctuations. First of all, the variation of FWHM in Fig. 3 occurs in an extent of around 5.2 meV, 14.9 meV, 18.8 meV, and 35.1 meV for samples S120, S160, S200, and S240, respectively, which indicates an increase of the variation range of FWHM with increasing well width. Here, the above values are the differences between the maximum and the minimum values in these curves. As for the origin of enhancement in carrier localization, it may be attributed to the thickness fluctuations in the InGaN/GaN MQWs. The possible reasons for the thickness fluctuations may be ascribed to the increasing interface roughness and strains between the well and the barrier layers with increasing well width,[8] since growing a thick well using a long growth time could easily form worse interfaces between the wells and the barriers. It is also found from the temperature-dependent FWHM that, for S160, S200, and S240, the FWHM decreases slightly at first and then increases continuously up to room temperature. The initial decrease is the consequence of carriers randomly distributed in all localization states at very low temperature relaxing down into lower localized states via hopping due to increasing temperature.[22] With further increasing temperature, the carriers can approach the thermal equilibrium with the lattice. The localized carriers are easily excited out from lower localization states to higher localization states or nonradiative recombination centers, resulting in a broadening of the PL spectra. However, for S120, at intermediate temperatures (120–180 K), there is a slight reduction in FWHM with the increase of temperature. In the intermediate temperatures, due to the relatively weak localization effect in sample S120, most localized carriers, even carriers in the deepest localization centers, become progressively mobile.[20] Therefore the carrier distribution narrows when most of the carriers in lower localization states tend to transfer into higher localization states, and thus a reduction of FWHM occurs. Above the intermediate temperature region, the role of the regular thermalization of carriers starts to become more and more important, leading to an increase of FWHM. In addition, it can be seen from Fig. 3 that, for sample S200, the turnover from the first decrease to increase appears at relatively higher temperature (about 125 K), while for the other three samples it appears at about 60 K. It means that, in S200, the localized carriers need more thermal energy to escape from the localized potential minima, which is in accordance with the fact that it has stronger localization effect than S120 and S160. It seems strange that, unlike S200, the turnover from the first decrease to increase in Fig. 3 for S240 occurs at low temperature in spite of the strong localization effect. It can be probably attributed to increasing defects with widening QW layers. Some literature[9,25] has experimentally confirmed this conclusion that thicker wells are prone to the generation of defects in the MQW structure since the QW thickness increases and even approaches to the critical thickness. On the one hand, since the nonradiative recombination process may be dominant because of the increased defects with increasing well width, the carrier life-time decreases at low temperature, giving the carriers less opportunity to relax down into the lower energy tail states. On the other hand, the heating effect may be significant due to the existence of more defects acting as nonradiative recombination centers in S240 with wider well. The serious heating effect can overcome the carrier confinement in the localization centers, which promotes the carriers in deeper localization states to escape from the deeper localization states even at low temperatures. Therefore the defects finally promote the escape of carriers from deep localization centers, leading to the occurrence of blueshift at low temperature.

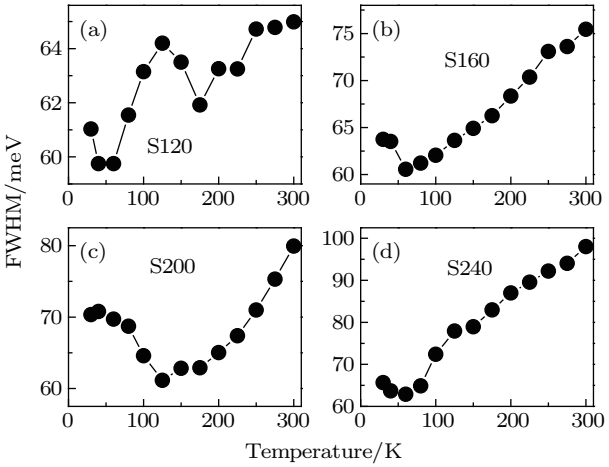


Fig. 3. Temperature-dependent FWHM for (a) S120, (b) S160, (c) S200, and (d) S240.

To analyze the broadening behavior of the PL spectra with increasing temperature and clearly check the variation of the spectral shape, the intensity of the temperature-dependent PL spectra of each sample is normalized and depicted in Fig. 4. As shown in Fig. 4, when the temperature exceeds the low temperature region, the PL spectral broadening increases with increasing temperature. In detail, the temperature-induced broadening always occurs mainly on the low-energy side of the PL spectra due to band-gap shrinkage at rising temperatures (as shown by the black arrows in Fig. 4), while the PL spectra on the high-energy side, especially in rectangular frames, stay nearly unchanged except for the case of S240 (as shown by the green arrow in Fig. 4(d)). Although the carriers are still excited out to higher localization states, the temperature induced band-gap shrinkage may be dominant and thus the broadening of the PL spectra occurs on the low-energy side for S120, S160, and S200. Therefore, for these three samples, the increase in

the FWHM comes mainly from a shift on the low-energy side of the PL spectra. However, except the extension on the low energy side, the PL spectra for S240 also extend on the high energy sides especially in rectangular frames. Because of the strongest potential fluctuations in S240 which has the widest well among the four samples, there may be a large number of shallow localization states in the band gap, in favor of a wider distribution of carriers into these shallow localization states at increasing temperature. It will lead to a remarkable extension of the PL spectra on the high-energy sides.

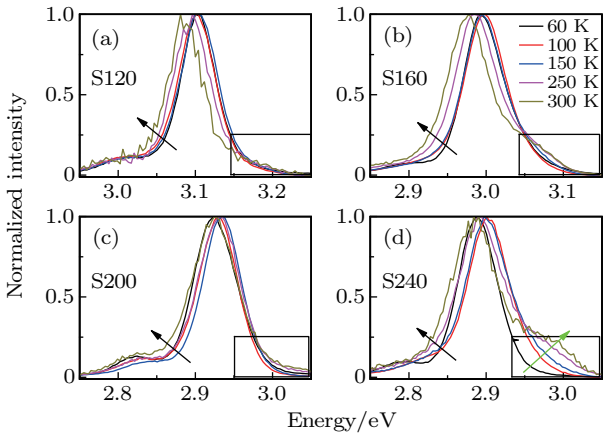


Fig. 4. (color online) The PL spectra of (a) S120, (b) S160, (c) S200, and (d) S240 at different temperatures. The PL peak intensity is normalized individually at each temperature. The arrows indicate the shift direction of the spectral curve when the temperature rises.

Based on the above discussion about the localization states, the PL spectra of these four samples can be better understood. As the well width increases, the number of photogenerated carriers increases due to increasing laser-absorbing active region volume. Also, the carrier localization effect is enhanced, so the carriers can be better confined in the localized states and form bound excitons, suppressing the possible nonradiative recombination at dislocations. Therefore, the PL intensity is increased when the well width increases from 1.8 nm to 3 nm. However, in spite of the increasing laser-absorbing active region volume and localization effect, the PL intensity is reduced after the well width reaches 3.6 nm. The reduced PL intensity may be attributed to the enhanced QCSE and the degraded material quality of the thicker InGaN layers.

4. Conclusions

In summary, the localization effect in blue-violet light emitting InGaN/GaN MQW structures with varying well width is investigated by temperature-dependent PL measurement. It is found that the carrier localization effect is enhanced with increasing well width from 1.8 nm to 3.6 nm in our experiments, which may be related to the increased thickness fluctuations of the InGaN well layers. By comparing the localization effect and the linewidth variation of the PL peak, the study further shows that a greater amplitude of potential fluctuation as well as more localization states exist in MQW with wider wells. As for the temperature-induced broadening of the PL spectra, it is found that the shift of the spectral curves always mainly occurs on the low-energy side of the PL spectra, while in the case of the widest well, an extension occurs also at the high-energy sides. As a conclusion, due to the comprehensive effects of the localization effect, QCSE, the influence of the material quality of InGaN layers, and the laser-absorbing active region volume, a moderate well width will be favorable in improving PL quality.

References

[1] Ji P F, Liu N X, Wei X C, Liu Z, Lu H X, Wang J X and Li J M 2011 *J. Semicond.* **32** 103001
[2] Wang Q, Ji Z W, Wang F, Mu Q, Zheng Y J, Xu X G, Lu Y J and Feng Z H 2015 *Chin. Phys. B* **24** 024219
[3] Fu B L, Liu N X, Liu Z, Lu H X, Li J M and Wang J X 2014 *J. Semicond.* **35** 114007
[4] Li X, Liu Z S, Zhao D G, Jiang D S, Chen P, Zhu J J, Yang J, Le L C, Liu W, He X G, Li X J, Liang F, Zhang L Q, Liu J P and Yang H 2015 *Appl. Opt.* **54** 8706
[5] Ji X L, Yang F H, Wang J X, Duan R F, Ding K, Zeng Y P, Wang G H and Li J M 2010 *J. Semicond.* **31** 094009
[6] Sun Q, Yan W, Feng M X, Li Z C, Feng B, Zhao H M and Yang H 2016 *J. Semicond.* **37** 044006
[7] Cao K W, Fu B L, Liu Z, Zhao L X, Li J M and Wang J X 2016 *J. Semicond.* **37** 014008
[8] Ko T S, Lu T C, Wang T C, Chen J R, Gao R C, Lo M H, Kuo H C, Wang S C and Shen J L 2008 *J. Appl. Phys.* **104** 093106
[9] Liu W, Zhao D G, Jiang D S, Chen P, Liu Z S, Zhu J J, Shi M, Zhao D M, Li X, Liu J P, Zhang S M, Wang H and Yang H 2015 *J. Alloys Compd.* **625** 266
[10] Schomig H, Halm S, Forchel A and Bacher G 2004 *Phys. Rev. Lett.* **92** 1506802
[11] Narukawa Y, Kawakami Y, Fujita S, Fujita S and Nakamura S 1997 *Phys. Rev. B* **55** 55
[12] Na J H, Taylor R A and Lee K H 2006 *Appl. Phys. Lett.* **89** 253120
[13] Bai J, Wang T and Sakai S 2000 *J. Appl. Phys.* **88** 4729
[14] Zhao K, Yang X, Xu B, Li D, Wang C and Feng L 2016 *J. Electron. Mater.* **45** 786
[15] Wang T, Nakagawa D, Lachab M, Sugahara T and Sakai S 1999 *Appl. Phys. Lett.* **74** 3128
[16] Li Z, Kang J, Wang B W, Li H, Weng Y H, Lee Y C, Liu Z, Yi X, Feng Z C and Wang G 2014 *J. Appl. Phys.* **115** 083112
[17] Mohanta A, Wang S F, Young T F, Yeh P H, Ling D C, Lee M E and Jang D 2015 *J. Appl. Phys.* **117** 144503
[18] Hoffmann V, Mogilatenko A, Netzel C, Zeimer U, Einfeldt S, Weyers M and Kneissl M 2014 *J. Cryst. Growth* **391** 46
[19] Zhao D G, Jiang D S, Zhu J J, Wang H, Liu Z S, Zhang S M, Wang Y T, Jia Q J and Yang H 2010 *J. Alloys Compd.* **489** 461
[20] Wang H, Ji Z, Qu S, Wang G, Jiang Y, Liu B, Xu X and Mino H 2012 *Opt. Express* **20** 3932
[21] Langer T, Pietscher H G, Ketzer F A, Jonen H, Bremers H, Rossow U, Menzel D and Hangleiter A 2014 *Phys. Rev. B* **90** 205302
[22] Liu W, Zhao D G, Jiang D S, Chen P, Liu Z S, Zhu J J, Shi M, Zhao D M, Li X, Liu J P, Zhang S M, Wang H, Yang H, Zhang Y T and Du G T 2015 *Opt. Express* **23** 15934
[23] Eliseev P G, Perlin P, Lee J and Osiński M 1997 *Appl. Phys. Lett.* **71** 569
[24] Eliseev P G, Osinski M, Lee J, Sugahara T and Sakai S 2000 *J. Electron. Mater.* **29** 332
[25] Redaelli L, Mukhtarova A, Valdueza-Felip S, Ajay A, Bougerol C, Himwas C, Faure-Vincent J, Durand C, Eymery J and Monroy E 2014 *Appl. Phys. Lett.* **105** 131105